

# Preparation and Characterization of Aerogels Derived from $\text{Al}(\text{OH})_3$ and $\text{CrO}_3$

Michael R. Ayers, Ashley A. White, Xiang-Yun Song, and Arlon J. Hunt\*

*E.O. Lawrence Berkeley National Laboratory, Berkeley, CA, 94720, USA*

## Abstract

Aerogels containing both  $\text{Al}_2\text{O}_3$  and  $\text{Cr}_2\text{O}_3$  were prepared by the reduction, by alcohols, of a precursor salt solution derived from  $\text{Al}(\text{OH})_3$  and  $\text{CrO}_3$ , followed by supercritical drying in either  $\text{CO}_2$  or ethanol. TEM analyses showed a microstructure typical of aerogels, with a connected matrix of  $\sim 10$  nm-diameter particles and an open pore network. Subsequent thermal processing converts the initial aerogels to a high surface-area material comprised of  $\text{Al}_2\text{O}_3$  and  $\text{Cr}_2\text{O}_3$ . Addition of  $\sim 6\%$   $\text{SiO}_2$ , relative to Al results in an increased retention of surface area at high temperatures. Surface areas of the aerogels after supercritical drying ranged from 240 to  $700 \text{ m}^2/\text{g}$ , while after treatment at  $1000^\circ\text{C}$  values ranged from 110 to  $170 \text{ m}^2/\text{g}$ . The composition which showed the greatest temperature stability was  $2(0.94\text{Al}_2\text{O}_3 \cdot 0.06\text{SiO}_2)\text{Cr}_2\text{O}_3$ . After treatment at  $1000^\circ\text{C}$ , all a samples contained a large number of crystallites of the  $\text{Cr}_2\text{O}_3$  phase, eskolaite, with diameters ranging from 0.5 to  $1.0 \mu\text{m}$ . An additional unidentified phase may also be present. The presence of these larger crystallites leads to a lower transmittance in the near-IR due to increased scattering.

*PACS Codes:* 81.05.R, 61.43.G, 81.20.F

\*Corresponding author. Tel: +1-510-486-5370; fax: +1-510-486-7303; e-mail: [ajhunt@lbl.gov](mailto:ajhunt@lbl.gov)

## 1. Introduction

Alumina- and chromia-based materials with a high surface areas and open porosity are attractive materials for uses requiring a low thermal conductivity at high temperatures [1], or a stable microstructure for catalytic reactions [2-7]. Such nanostructured oxides may lead to performance or efficiency improvements in both of these areas. In industrial heating applications, advanced porous materials would be expected to lower the thermal conductivity of refractory bricks or backing insulations, thereby significantly reducing energy consumption. While for applications in catalysis, high surface areas and thermal stability give increased turnovers and yields in many cases. Synthesis and drying procedures leading to  $\text{Al}_2\text{O}_3$  and  $\text{Cr}_2\text{O}_3$  aerogels, as either primary or binary oxides, have been available for some time. Alumina aerogels are most commonly prepared by a standard sol-gel approach through the hydrolysis and condensation of a sterically hindered aluminum alkoxide, such as an *s*-butoxide, or an acetylacetonate [8-11]. However, there has been one recent report of the preparation of alumina aerogels by the reaction of aluminum nitrate with propylene oxide [12]. The use of alkoxide precursors is problematic due to their extreme cost and low ceramic yield. Chromia aerogels have been prepared by the reduction of  $\text{CrO}_3$  by alcohols [13].

With the aim of developing a straightforward preparation of alumina-chromia aerogels from low-cost precursors, we report here the syntheses of such materials derived from  $\text{Al}(\text{OH})_3$  and  $\text{CrO}_3$ . These reagents react smoothly, by an acid-base process, to form a highly soluble salt which is available for further reduction by alcohols, yielding rigid gels. A further aim of this work was to determine the composition and processing conditions that lead to retention of a high surface area and porosity after exposure to high temperatures. In this regard, it has long been known that incorporation of a small percentage of  $\text{SiO}_2$  into alumina aerogels greatly reduced their

loss of surface area upon thermal exposure [14,15]. Therefore, we have also studied ternary oxides of the  $\text{Al}_2\text{O}_3/\text{Cr}_2\text{O}_3/\text{SiO}_2$  system. The physical properties of these materials after conversion to aerogels by supercritical drying, and after subsequent treatment at high temperatures will be discussed.

## 2. Experimental procedures

$\text{Al}(\text{OH})_3$ ,  $\text{CrO}_3$  (99%), and tetramethoxysilane (TMOS) were purchased, and used as received, from Aldrich Chemical Corp. Freshly-obtained quantities of the alkoxides tetraethoxysilane (TEOS, EM Science,) Aluminum di(sec-butoxide)acetoacetic ester chelate (Alfa Aesar, Tech Grade,) diethoxysilane-sec-butylaluminate copolymer (Gelest, Inc.,) and polyethoxysilane (Silbond Corp., H-5 Grade) were used in all cases. Polyethyleneglycol (PEG-300) was obtained from Dow Chemical Corp. Methanol, ethanol, 2-propanol, and 1-butanol were obtained from various sources as anhydrous solvents and used without further purification.

Single-point BET surface area measurements were obtained using a Quantasorb surface analyzer (Quantachrome, Inc.) from the desorption of 30%  $\text{N}_2/\text{He}$ . Helium pycnometry and multi-point BJH pore size distributions were performed by the Micromeritics Materials Analysis Laboratory (Norcross, GA, USA.) A TA Instruments SDT 2960 TGA-DTA system was used for thermal analyses. X-ray diffraction powder patterns were collected on a Siemens Kristalloflex diffractometer using  $\text{Cu K}\alpha$  radiation. Samples for TEM analyses were ground, suspended in acetone, and evaporated onto holey carbon-Cu grids. TEM images were taken with either a Topcon 002B microscope at 200 kV, or a JEOL 200CX analytical microscope with an ultrathin-window EDX attachment, operating at 200 kV. Near-IR transmission measurements

were obtained with a Nicolet Magna-IR 760 spectrophotometer, using 3 % (w/w) dispersions of the analyte in mineral oil.

Thermal treatment of dried aerogel samples was carried out in a box furnace under air, unless otherwise indicated. All samples were held at the desired temperature for 60 minutes.

Preparation of wet gels derived from aluminum hydroxide followed the following general procedure, using the reagent quantities listed in Table 1. The desired amounts of  $\text{Al}(\text{OH})_3$  and  $\text{CrO}_3$  were placed in a tall-form beaker, to which a mixture of  $\text{H}_2\text{O}/17\text{N HNO}_3$  was added. The exothermic reaction between the acidic  $\text{CrO}_3$  and  $\text{HNO}_3$  and basic  $\text{Al}(\text{OH})_3$  began instantly, and after 1-2 minutes of slow stirring the mixture existed as a bright orange suspension. At this point, samples were placed on a hot plate and gently heated for 20-30 minutes. During this stage, gas was released and the suspension changed to a deep red, highly viscous Al-Cr salt solution with no solids visible. This process was judged to be complete when the evolution of gas had ceased, but the solution was still thin enough to be stirred.

The stirring rate was then increased and the desired amount of alcohol was quickly added. If silica was desired in the final product, the silicon alkoxide precursor was dissolved in the alcohol prior to mixing with the Al-Cr salt solution. The reduction of the chromium IV present began immediately, forming a dark brown solution. Care was taken to ensure that all of the Al-Cr salt solution was dispersed before gelation, which, depending on the sol density, occurred in as fast as 30 seconds to over 3 hours.

The gels were then covered and placed in a sealed container under a saturated ethanol atmosphere to age for 24 hours. The gels were often quite rigid, though their strength varied considerably in proportion to the original sol density. Most of the gels were dark brown in color, however, gels derived from very low density sols often appeared slightly green. After aging, the

gels were removed from their containers and soaked in anhydrous ethanol in a bath of at least ten times the gel volume for 24 hours. This soaking procedure was then repeated an additional two times. Though quite brittle, with great care the gels could often be removed from their containers as monolithic pieces. However, for convenience of handling and drying they were typically allowed to break into smaller pieces of about 1 cm<sup>3</sup> in size.

To evaluate the effect of high temperature prior to drying on the final aerogel's properties, one sample was soaked in 20 volumes of PEG-300 for 7 days. The sample was then heated to 185 °C for 180 minutes, during which time its color changed from brown to dark green. This sample was then exposed to a second set of three 24-hour alcohol soaks to remove the PEG-300 before supercritical drying.

Drying of the wet gels, to produce the corresponding aerogels, followed standard CO<sub>2</sub> substitution and drying procedures [16]. The total process time was 18 hours, and the process conditions were maintained at 5 °C and 55 bar during the substitution phase, and 45 °C and 90 bar during the drying phase. The aerogels generally appeared dark green-brown to black and were effectively opaque. Shrinkage of the gels during this stage was relatively slight, and the samples maintained ~60-70% of their original volume.

For comparison, one sample was dried using the supercritical ethanol method. A 25 mL piece of this sample along with an additional 20 mL of ethanol, was placed in a 200-mL vessel which was then pressurized to 67 bar with dry nitrogen. The vessel was heated to 300 °C over a 45 minute period, and the pressure was maintained at 67 bar by venting the contents when needed. The system was held at this temperature for 30 minutes and was then slowly vented to ambient pressure. The aerogels dried in this way were dark green, and exhibited slightly more shrinkage than their CO<sub>2</sub>-dried counterparts, retaining only ~40-50% of their original volume.

An aerogel derived from alkoxide precursors and  $\text{CrO}_3$  was also prepared for comparative purposes. This sample (F1) was prepared by mixing 30 g (29.1 mL, 0.1 mol) Aluminum di(sec-butoxide)acetoacetic ester chelate, 2.25 g (~2.2 mL, ~0.006 mol Al/0.0056 mol Si) diethoxysilane-sec-butylaluminate copolymer, and 220 mL of ethanol to which 5.0 g (0.05 mol)  $\text{CrO}_3$  dissolved in 30 mL of water was added with vigorous stirring. The mixture formed a rigid brown gel within 1-2 minutes. The gels were then aged for 24 hours, followed by a soaking procedure as described above, and dried using the  $\text{CO}_2$  method.

### 3. Results

The specific surface areas of the various gels studied here are summarized in Table 1. Several sets of gel recipes were evaluated to determine the composition which maintained the highest surface area after exposure to high temperatures. Series A evaluated the effect of the Al/Cr ratio, which produced a considerable variation in the final surface areas. The unbaked aerogels gave the highest surface area when Al/Cr was low, though the values were fairly similar. After heating to 450 °C, the temperature at which most of the mass loss has already occurred, a this trend is continued, with the notable exception of the aluminum-free sample A1 that has lost the majority of its surface area. However, after heating to 1000 °C, the trend reverses, and the samples with the highest Al/Cr retain the most surface area.

The effect of the addition of 6% (mol/mol) silica, relative to alumina, from various silicon alkoxide precursors is shown in series B. In all cases the addition of silica results in a significant increase in the surface area of the freshly dried aerogel, and a large increase, of around 2X, in the surface area after baking at 1000 °C.

Series C shows the effect of the type of alcohol used as solvent and reductant for the gelation. The variation is not large, however ethanol gives the highest value for both the original aerogel ( $420 \text{ m}^2/\text{g}$ ) and for the sample after baking at  $1000^\circ\text{C}$  ( $130 \text{ m}^2/\text{g}$ ).

Additionally, three special cases were also measured. A gel prepared by the recipe of sample C2, but heated to  $185^\circ\text{C}$  in PEG-300 (sample D1), possessed a relatively low surface area in both the original aerogel ( $240 \text{ m}^2/\text{g}$ ), and the aerogel baked at  $1000^\circ\text{C}$  ( $110 \text{ m}^2/\text{g}$ ). Sample E1, with the same composition as C2, but dried using supercritical ethanol, gave the highest surface areas of any aerogel measured,  $700 \text{ m}^2/\text{g}$  for the original aerogel, and  $170 \text{ m}^2/\text{g}$  after baking at  $1000^\circ\text{C}$ . Finally, the alkoxide-derived aerogel gave surface area results comparable to those of the samples from series C.

The effect of high temperatures on the alumina-chromia aerogels is revealed by the TGA plots shown in Fig. 1. Both the aerogel derived from  $\text{Al}(\text{OH})_3$ , sample C2, and the alkoxide-derived gel, F1, show most of their mass loss at relatively low temperatures with the majority occurring below  $400^\circ\text{C}$ . Sample C2 retains approximately 47% of its mass after heating to  $1000^\circ\text{C}$ , while sample F1 shows a somewhat higher mass retention of 55%.

The skeletal densities of sample C2 before and after thermal treatments, were determined by helium pycnometry. The original aerogel, gave a value of  $1.92 \text{ g}/\text{cm}^3$ , while the same sample baked at  $450^\circ\text{C}$  had increased to  $2.69 \text{ g}/\text{cm}^3$  and the sample taken to  $1000^\circ\text{C}$  to  $3.59 \text{ g}/\text{cm}^3$ . The value for the thermally-treated sample is somewhat less than might be expected for a mixture of alumina ( $3.9 \text{ g}/\text{cm}^3$ ) and chromia ( $5.2 \text{ g}/\text{cm}^3$ ), suggesting the presence of closed porosity.

Figure 2 gives examples of TEM images of sample C2. In the top image, of the original aerogel, a structure common to many aerogel material is observed. Irregularly shaped primary

particles with dimension on the scale of 10-20 nm, are linked in an extended network surrounding regions of open porosity. After baking at 1000 °C, a considerable change in structure is evident as seen in the bottom image. The porous network of small particles is still present, but a considerable coarsening of the particle size and closure of much of the porosity is evident. More significant, however, is the presence of large crystallites within the aerogel network. These appear fairly evenly distributed throughout the sample and were consistently observed in many micrographs. The images suggest two morphologies, however, this can not be determined conclusively. Circular, or oblong, shapes with diameters approaching 1  $\mu\text{m}$  are common. Smaller, rod-shaped object are also readily seen, with lengths on the order of 0.5  $\mu\text{m}$ . It is possible, however, that there is only one morphology, approximating platelets, and the objects that appears as rods are actually these platelets viewed edge-on.

Figure 3 shows TEM images of the alkoxide-derived aerogel (F1), for comparison. The microstructure of both the original aerogel, and the aerogel after baking at 1000 °C show many similarities to the microstructure of the aerogels derived from  $\text{Al}(\text{OH})_3$ . The original aerogel does exhibit a somewhat finer primary particle size, relative to sample C2, though their surface areas are fairly similar. This suggest that the primary particles in the  $\text{Al}(\text{OH})_3$ -derived aerogels may contain a considerable amount of microporosity. However, the most noticeable difference between the  $\text{Al}(\text{OH})_3$ - and alkoxide-derived aerogels is the lower number of larger crystallites seen in the latter case after baking at 1000 °C. Such crystals were formed in sample F1, as seen in Fig. 3, though only one morphology was observed.

Pore size distribution curves derived from nitrogen desorption isotherms appear in Fig. 4a-c. Aerogels of sample C2 without thermal treatment and after baking at 450 °C and 1000 °C are shown in Fig. 4a. The peak of the pore volume curves is at 20-30 nm in all three cases,



however, a steady loss of pores with diameters  $<10$  nm is seen as the baking temperature is increased. This effect is more drastically seen in Fig. 4b, which shows the pore distribution for sample E1, the sample dried using the supercritical ethanol method. In this case the unbaked aerogel contains a much higher fraction of pores with diameters  $<10$  nm, though the peak of the distribution is again in the range of 20-40 nm. After heating at 1000 °C, most of the small pores have been lost, as well as a considerable fraction of the overall porosity. The peak of the distribution remains at  $\sim 25$  nm, however. Finally, Fig. 4c gives the pore distribution curves for aerogel sample D1, the sample that was heated in PEG prior to supercritical drying. An overall lower porosity is observed in both the unbaked aerogel and the aerogel after baking at 1000 °C, relative to the previous samples. The peak distribution for the unbaked aerogel again falls between 20-50 nm, and a significant amount of  $<10$  nm pores are also seen. After baking the peak of the distribution curve has shifted slightly, to  $\sim 30$  nm, and the small pores have once again been lost.

The distribution of chemical species within the aerogel samples was evaluated using EDX spectroscopy. Sample C2 was investigated both as the original aerogel, and after baking at 1000 °C. The unbaked aerogel, examined at many points, showed a fairly consistent distribution of Al and Cr throughout the sample. The number of counts for the Al peak is typically 1.5 times that of the main Cr peak. In the case of the heat treated sample, however, the TEM results suggested a considerable inhomogeneity. In regions where the sample consists of a microporous aerogel-like structure, the ratio of Al to Cr is much higher, with the number of counts for Al typically 4 times that of Cr. For the larger crystallites, the EDX spectra are shown in Fig 5. The top spectra in Fig. 5 corresponds to point A in Fig. 2, a point taken over one of the larger irregularly-shaped crystallites. In this case the Cr peak dominates the spectrum, showing almost

5 times the counts as the Al peak. However, the rod-shaped crystallites shows the reverse case, with the Al peak giving ~2 times the counts as the Cr peak, as seen in the bottom spectrum of Fig. 5. This shows that a significant amount of phase segregation occurs as the aerogel is exposed to high temperatures, with Cr migrating out of the microstructured aerogel-like areas of the sample and into the newly-formed large particles. These spectra also suggest that the two particle morphologies observed by TEM may indeed represent different chemical species. However, the effect of the aerogel-like material, which may entirely surround the crystallites, may introduce uncertainty into these measurements.

To better elucidate the nature of the crystalline species present after treatment at 1000 °C, XRD patterns were obtained, and these appear in Fig. 6. Patterns for sample C2, D1, and F1 all show one major phase, the  $\text{Cr}_2\text{O}_3$  phase, eskolaite. Sample C2 does not exhibit any additional peaks or features other than those for eskolaite. The sample heated in PEG, D1, does not show additional strong peaks, but does possess broad feature at low angles ( $20 < 2\theta < 40$ ) with a greater intensity relative to sample C2. This feature is commonly seen in the XRD patterns of amorphous aerogel materials. The pattern for sample F1, the alkoxide-derived aerogel, shows additional peaks at  $2\theta = 30, 35$  and  $63$  degrees. These peaks exhibit some similarities to the  $\text{SiO}_2$  phase, shistovite, however the match is not exact. The pattern for the ethanol-dried sample E1, was virtually identical to that of its  $\text{CO}_2$ -dried counterpart, sample C2. Sample C2 does not show any patterns which could be attributed to a second, aluminum-rich, crystalline phase as suggested by the EDX analysis. However, literature patterns for  $\text{Al}_{1.4}\text{Si}_{0.3}\text{O}_{2.7}$ , a phase with a similar Al to Si ratio to that of sample C2, shows only two XRD peaks, at  $2\theta = 24.5$  and  $66$  degrees. Since these peaks would potentially be covered by two eskolaite peaks at approximately the same position, the existence of this phase can not be ruled out.

The presence of larger crystallites in the aerogels after exposure to high temperatures suggests that these materials may show a lower transparency in the near infrared, due to increased scattering by these inhomogeneities. The near-IR spectra of samples C2 and F1 appear in Fig 7. Sample C2, with a higher proportion of larger crystallites, as determined by TEM, shows a more significant decrease of transmittance at shorter wavelengths, relative to sample F1. The absolute transmittance of sample C2 is lower and the slope of the spectrum is greater in the region from 8000 to 5000  $\text{cm}^{-1}$ . This indicates a decrease in transparency at these frequencies, corresponding to the higher number of large crystallites in this sample.

#### **4. Discussion**

The reaction between  $\text{Al}(\text{OH})_3$  and  $\text{CrO}_3$  provides a convenient precursor to aerogels containing both  $\text{Al}_2\text{O}_3$  and  $\text{Cr}_2\text{O}_3$ . The ratios of these oxides can be varied over a fairly wide range without drastically affecting the ability of the precursor solution to form a rigid gel. However, it was found that the addition of one equivalent of  $\text{HNO}_3$ , relative to  $\text{Al}(\text{OH})_3$  yields gels with greatly improved homogeneity and stiffness. The critical aspect to the syntheses of good-quality gels is allowing the initial reaction of  $\text{Al}(\text{OH})_3$  and  $\text{CrO}_3$  to go to completion before attempting the reduction with alcohol. If the reduction is attempted too early, such as when solids are still present in the mixture, the sol will not gel but will form precipitates. Timing this step of the synthesis properly is, therefore, quite important. As mentioned above, the evolution of gas should have ceased before reduction, but the mixture should still possess a viscosity that allows it

to be stirred. The nature of the gas evolved in this step was not determined in this study, however it is likely  $O_2$  released by the conversion of  $CrO_4^{2-}$  to  $Cr_2O_7^{2-}$ .

The reduction step proceeds smoothly if the salt solution precursor has been prepared properly. Various alcohols can be used for this step, and it is likely that many other species can serve as both solvent and reductant as well. The solids content of the wet gel can be varied somewhat by adjusting the amount of alcohol used. Relative to sample C2, rigid gels could be prepared with twice the solids content by using half as much alcohol. Preparing very low solids content gels was somewhat more limited in scope. The practical lower limit for solids content, below which the sols would not gel, was approximately 45% that of sample C2, and was achieved by increasing the volume of alcohol used by the corresponding amount.

Drying the wet gels to produce the corresponding aerogels is straightforward using either the low-temperature  $CO_2$  substitution method, or the high temperature supercritical ethanol method. When  $CO_2$  drying is used, there is a very modest amount of shrinkage to 50-70% of the original volume, and the gels appear dark brown to black. The absolute amount of shrinkage is difficult to determine, due to the irregular shapes of the aerogel pieces. When ethanol drying is used, the shrinkage is higher, to perhaps 30-50% of the original volume, and the aerogel is now dark green in color. This indicates that the conversion of  $CrO_2$ , the initial product of the reduction of  $Cr^{VI}$ , to  $Cr_2O_3$  has begun during the drying stage. This was also observed in sample D1, during its pre-drying heat treatment in PEG-300.

Thermally treating the aerogels produced in this way leads to loss of around 50% of the original mass of the sample. This results from the loss of several volatile species evolved as the aerogel is heated. The chemical nature of the species presumed to be present at various stages of this process are as follows. The precursor salt solution, for the composition used in sample C2

and omitting the small fraction of silica present for clarity, is comprised of  $2[\text{Al}(\text{OH})^{2+}] \cdot [\text{CrO}_4 \cdot 2(\text{NO}_3)]^{4-}$ , or a similar formula containing dichromate ions. After reduction by alcohol, the gels likely consist of,  $2[\text{Al}(\text{OH})(\text{NO}_3)]\text{O} \cdot \text{CrO}_2$ . High temperature treatment of this material, would release water from the condensation of -OH groups,  $\text{NO}_2$  from the pyrolysis of - $\text{NO}_3$  groups, and  $\text{O}_2$  from the conversion of  $\text{CrO}_2$  to  $\text{Cr}_2\text{O}_3$ . This would account for a mass loss of only 27%. The higher observed mass loss of 55% may then result from the loss of free water or alcohol trapped in the aerogel matrix, or possibly from the loss of - $\text{CO}_3$  groups that could be formed during  $\text{CO}_2$  drying.

The desirable physical properties for a material of this type when used in high temperature applications, would be a stable microstructure with a high surface area, and an open pore network of with a high total pore volume. With regards to maintaining a high surface area the composition of sample C2 produces the best results. The addition of approximately 6% silica, relative to alumina, and use of a high Al/Cr ratio are the key factors in maintaining the surface area of the aerogel when exposed to high temperatures. The use of TMOS as the silica source, as in sample C1, does lead to a higher surface area, but the effect is not large, and does not outweigh the cost and safety advantages of using TEOS.

The production of aerogels that maintain a very low density after thermal treatments proved to be more problematic. Gels with lower solids content could be synthesized. However, due to the generally weaker solid network in these cases, the gels exhibited slightly more shrinkage during supercritical drying, and much more after exposure to high temperatures. This gives the result that aerogels produced from gels with low solids content and those prepared from gels with higher solids contents lead to aerogels with similar bulk densities after thermal treatment. The observed bulk volume of the aerogels after heating to 1000 °C was generally no

more than 10-15% of the volume of the original wet gel. Heating the aerogels under alternate atmospheres, such as argon, 100% O<sub>2</sub>, or vacuum did not significantly, or reproducibly affect the loss of porosity and shrinkage of the aerogels.

The pore size analyses of the aerogels produced here do not provide a complete understanding of the changes to their pore structures upon heating the samples. A distinctive feature of the changes seen in the aerogels is the loss of small pores with diameters <10 nm. This was seen in all cases, most notably in the sample dried using supercritical ethanol (E1). In that sample a very high number of small pores were present initially. This may have resulted from the initial protection of this porosity by the formation of -OEt groups via esterification reactions during drying. This effect is known to occur during the alcohol drying of silica aerogels and can restrict pore collapse by blocking surface condensation reactions. However, if this occurred in sample E1, its subsequent exposure to high temperatures would lead to removal of these -OEt groups and loss of porosity.

The loss of small pores can not account for the entire loss of bulk volume observed upon heating the aerogels. The total pore volume for sample C2 after heating to 1000 °C was still 66% of that of the original aerogel, as measured by N<sub>2</sub> adsorption. Additionally, the peak of the pore size distribution curve remains largely unchanged, near 25 nm. This suggests that the high shrinkage seen in these aerogels results from the loss of very large pores, with sizes not detected by gas adsorption methods.

The surface areas for these aerogels are typically maintained in the range of 100-150 m<sup>2</sup>/g after heating to 1000 °C for 60 minutes. This is similar to alumina-silica aerogels prepared by other methods. However, the presence of larger crystallites with dimensions on the order of 0.5-1.0 µm must lead to a lower average surface area. Therefore, the actual surface area of the finer-

structured portion of these aerogels, consisting of alumina-rich nanoparticles, must be considerably higher.

The formation of large crystallites of eskolaite,  $\text{Cr}_2\text{O}_3$ , provides insight into the structure of the original gel formed upon reduction of the precursor salt solution.  $\text{Al}_2\text{O}_3$  and  $\text{Cr}_2\text{O}_3$  show a high mutual solubility and the fact that large crystallites of  $\text{Cr}_2\text{O}_3$  form at high temperatures reveals a significant phase segregation must be present in the original wet gel. It is, therefore, likely that the gelation of  $\text{CrO}_2$ , being the daughter species of the primary reaction of chromate with alcohol, occurs first. This is followed by precipitation and gelation of the aluminum salt, which is no longer soluble after the removal of the chromate, or dichromate, counterion. TEM images of the original aerogel do not show a large distribution of particle sizes, so if the gelation does occur in two steps, the scale of the two networks must be similar. The network of  $\text{CrO}_2$  particles can then coalesce into larger particles upon heating. This is demonstrated by sample A1, which does not contain aluminum, and shows a decrease in surface area from 290 to 13  $\text{m}^2/\text{g}$  after heating to 1000 °C.

The formation of larger crystallites may, however, provide advantages if these aerogels are to be used in high temperature insulation applications. The transmission of thermal energy through radiation greatly outweighs the contribution of solid and gaseous conductivity at high temperatures. Therefore, radiation must be blocked by adsorption, scattering, or reflection for an insulation to be effective at these conditions. The oxides  $\text{Al}_2\text{O}_3$  and  $\text{Cr}_2\text{O}_3$  are reasonably transparent in the IR, especially at shorter wavelengths, which are dominant in the blackbody emission at temperatures of 1000 °C and above. Because of this, insulations based on these, or other, nanoporous oxides typically include an additional phase with larger dimensions to enhance the scattering of the transmitted light and increase their opacity. In the case of the aerogels

produced here, a larger-scaled feature is already present within the nanoporous network. This results in these materials showing a significant degree of self-opacification in the near-IR. This can be seen in Fig. 7, where the thermally treated aerogel derived from sample C2, with a large number of included crystallites, shows a lower transmittance compared to sample F1, derived from alkoxide precursors, with a lower number of crystallites. Further modifications to the synthesis and drying procedures to produce aerogels which retain a very low density after heat treatment, could yield materials with an exceptionally low thermal conductivity at high temperatures.

## 5. Conclusions

Aerogels containing both  $\text{Al}_2\text{O}_3$  and  $\text{Cr}_2\text{O}_3$  may be conveniently prepared by the reduction, by alcohols, of a precursor salt solution derived from  $\text{Al}(\text{OH})_3$  and  $\text{CrO}_3$ , followed by supercritical drying in either  $\text{CO}_2$  or ethanol. Subsequent thermal processing converts the initial aerogel to a highly porous, high surface-area material comprised of  $\text{Al}_2\text{O}_3$  and  $\text{Cr}_2\text{O}_3$ . The composition that retains the finest nanostructure after thermal treatment contains an Al/Cr ratio of 2:1, with an addition of ~6%  $\text{SiO}_2$ , relative to Al. Thermal treatment at high temperature leads to the crystallization of a portion of the solid network into particles with diameters of 0.5-1.0  $\mu\text{m}$ , with only one phase being positively identified as eskolaite,  $\text{Cr}_2\text{O}_3$ . Relative to supercritical drying in  $\text{CO}_2$ , drying in supercritical ethanol leads to a somewhat higher surface area., but does not reduce the total shrinkage combined from the drying and thermal post-treatment steps. Similarly, performing a thermal aging step in a high-boiling point solvent prior to supercritical  $\text{CO}_2$  drying gives a slightly lower surface area but also does not reduce the total shrinkage of the aerogel during drying and thermal processing. The samples prepared using various reagent ratios



and conditions consistently retained about 15-20% of the volume of the original wet gel after both supercritical drying and baking at 1000 °C.

However, the retention of a high surface area and a significant fraction of the original porosity after exposure to high temperatures, may allow these aerogel products to find uses as components of high temperature insulations, refractories, or catalysts. Use of these aerogel-derived materials in such applications will be greatly aided by the low costs of the raw materials used in this process. Both  $\text{Al}(\text{OH})_3$  and  $\text{CrO}_3$  are commodity chemicals, with costs orders of magnitude lower than the alkoxide-based precursors commonly used to synthesize aerogels by conventional sol-gel processes.

### **Acknowledgements**

This work was supported by the U.S. Dept. of Energy under contract No. DE-AC03-76SF00098 as part of the Office of Industrial Technologies-Industrial Materials of the Future Program.

## References

- [1] J.F. Poco, J.H. Satcher, L.W. Hrubesh, J. Non-Cryst. Solids. **285**, (2001) 57.
- [2] H. Hirashima, C. Kojima, H. Imai, J. Sol-Gel Sci. Tech. **8**, (1997) 843.
- [3] Y. Mizushima, M. Hori, J. Mater. Res. **10**, (1995) 1424.
- [4] H. Bozorgzadeh, E. Kemnitz, M. Nickkho-Amiry, T. Skapin, J.M. Winfield, J. Fluorine Chem. **110**, (2001) 181.
- [5] M.K. Younes, A. Ghorbel, Appl. Catal. A-Gen. **197**, (2000) 269.
- [6] J. Kirchnerova, D. Klvana, J. Chaouki, Appl. Catal. A-Gen. **196**, (2000) 191.
- [7] M.K. Younes, A. Ghorbel, C. Naccache, J. de Chim. Phys., Physico-Chimie Biol. **94**, (1997) 1993.
- [8] L. Le Bihan, F. Dumeignil, E. Payen, J. Grimblot, J. Sol-Gel Sci. Technol. **24**, (2002) 113.
- [9] J. Walendziewski, M. Stolarski, React. Kinet. Catal. Lett. **71**, (2000) 201.
- [10] A. Pierre, R. Begag, G. Pajonk, J. Mater. Sci. **34**, (1999) 4937.
- [11] K. Tadanaga, T. Iwami, T. Minami, N. Tohge, J. Ceram. Soc. Jap. **103**, (1995) 582.
- [12] A.E. Gash, T.M. Tillotson, J.H. Satcher, L.W. Hrubesh, R.L. Simpson, J. Non-Cryst. Solids. **285**, (2001) 22.
- [13] T. Skapin, J. Non-Cryst. Solids. **285**, (2001) 128.
- [14] B.E. Yoldas, J. Mater. Sci. **11**, (1976) 465.
- [15] T. Horiuchi, T. Osaki, T. Sugiyama, K. Suzuki, T. Mori, J. Non-Cryst. Solids. **291**, (2001) 187.
- [16] P.H. Tewari, A.J. Hunt, K.D Lofftus, **3**, (1985) 363.



## Figure Captions

**Figure 1.** TGA plots of (A) alumina-chromia aerogel derived from  $\text{Al}(\text{OH})_3$  (sample C2), and (B) from aluminum alkoxides (sample F1)

**Figure 2.** TEM micrographs of sample C2. Top: original aerogel without thermal treatment. Bottom: Same sample after baking at 1000 °C.

**Figure 3.** TEM micrographs of sample F1. Top: original aerogel without thermal treatment. Bottom: Same sample after baking at 1000 °C.

**Figure 4.** Pore size distribution plots of aerogel samples. **a:** Sample C2;  $\blacklozenge$  = original aerogel,  $\blacksquare$  = after baking at 450 °C,  $\bullet$  = after baking at 1000 °C **b:** Sample D1;  $\blacklozenge$  = original aerogel,  $\bullet$  = after baking at 1000 °C, **c:** Sample E1;  $\blacklozenge$  = original aerogel,  $\bullet$  = after baking at 1000 °C

**Figure 5.** EDX spectra of sample C2 after baking at 1000 °C. Top: Point in **Fig 2** marked by A. Bottom: Point in **Fig 2** marked by B

**Figure 6.** XRD patterns for aerogels after baking at 1000 °C. **A** = sample C2, **B** = sample F1, **C** = sample D1. Arrows above plot **C** correspond to literature patterns for the  $\text{Cr}_2\text{O}_3$  phase, eskolaite.

**Figure 7.** Near-IR spectra for aerogels after baking at 1000 °C. **A** = sample C2, **B** = sample F1.

**Table 1**

Reagent ratios for aerogel syntheses and surface area results.

Sample #	CrO <sub>3</sub> (mol)	Al(OH) <sub>3</sub> (mol)	HNO <sub>3</sub> (mol) in additional 4 mL H <sub>2</sub> O	Alcohol: 40 mL in each case	Silicon Alkoxide (mol)	Notes	Surface area (m <sup>2</sup> /g)		
							As dried	450 °C	1000 °C
A1	0.02	--	0.005	2-propanol	--	Very weak gel	290	13	13
A2	0.02	0.01	0.01	2-propanol	--		270	180	41
A3	0.02	0.02	0.02	2-propanol	--		260	160	44
A4	0.02	0.04	0.04	2-propanol	--	Rigid gel	240	170	64
B1	0.02	0.04	0.04	2-propanol	0.0024 TMOS	Brittle gel	350	--	130
B2	0.02	0.04	0.04	2-propanol	0.0024 TEOS	Rigid gel	300	--	120
B3	0.02	0.04	0.04	2-propanol	0.0024 polyethylsilicate	Brittle gel	530	--	110
C1	0.02	0.04	0.04	methanol	0.0024 TEOS		360	--	120
C2	0.02	0.04	0.04	ethanol	0.0024 TEOS		420	--	130
C3	0.02	0.04	0.04	2-propanol	0.0024 TEOS		300	--	120
C4	0.02	0.04	0.04	1-butanol	0.0024 TEOS	Soft gel	360	--	110
D1	0.02	0.04	0.04	ethanol	0.0024 TEOS	PEG heat treatment after gelation	240	--	110
E1	0.02	0.04	0.04	ethanol	0.0024 TEOS	Supercritical ethanol drying	700	--	170
F1	Alkoxide-derived aerogel, see text for reagent amounts						350	--	130

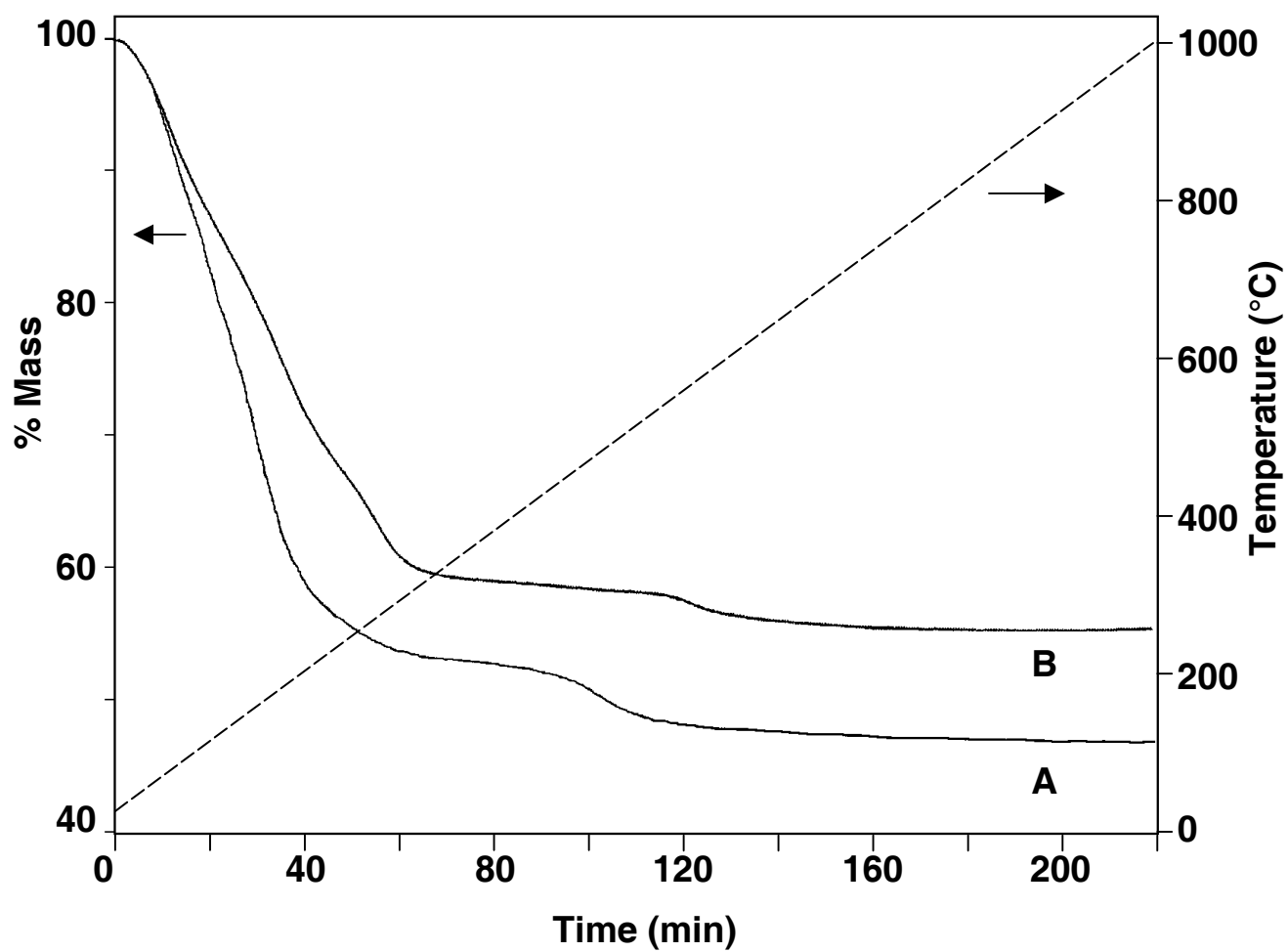


**Figure1** M. Ayers, et al. UP↑



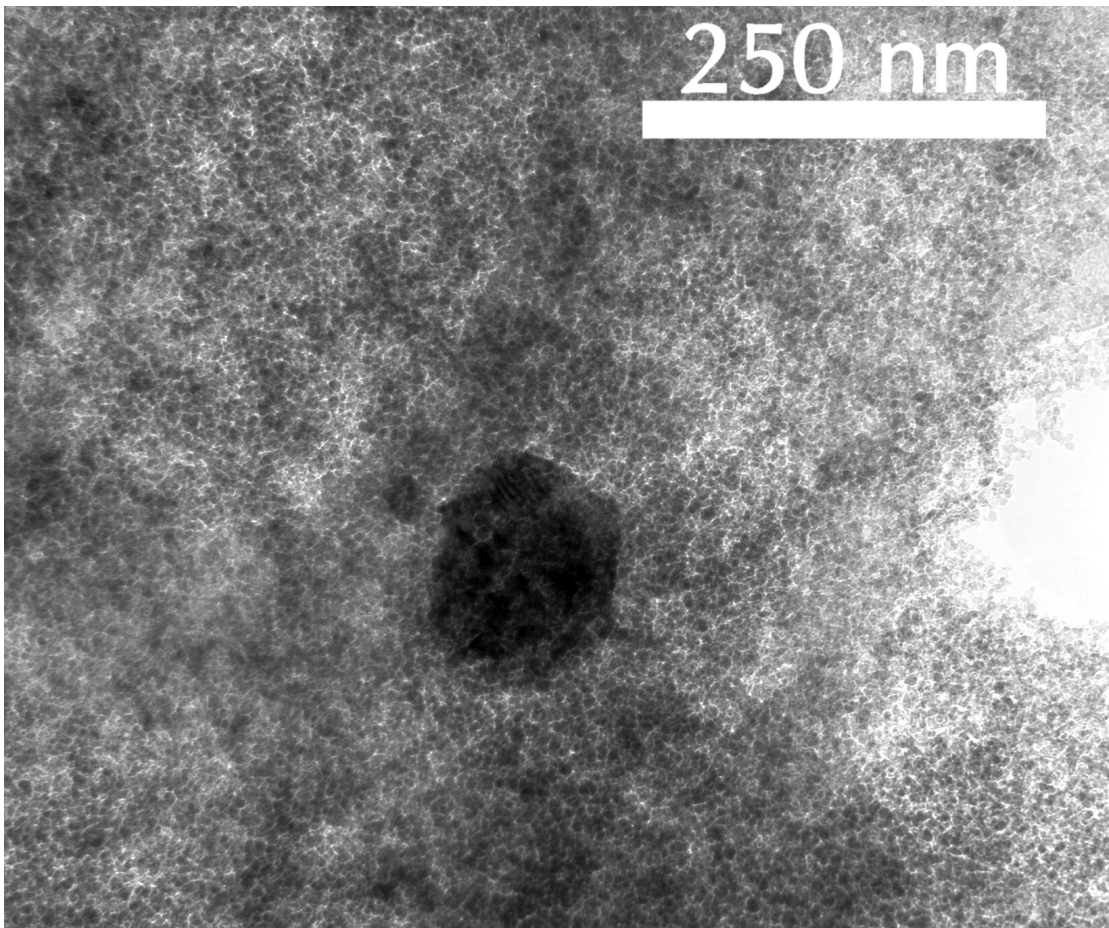
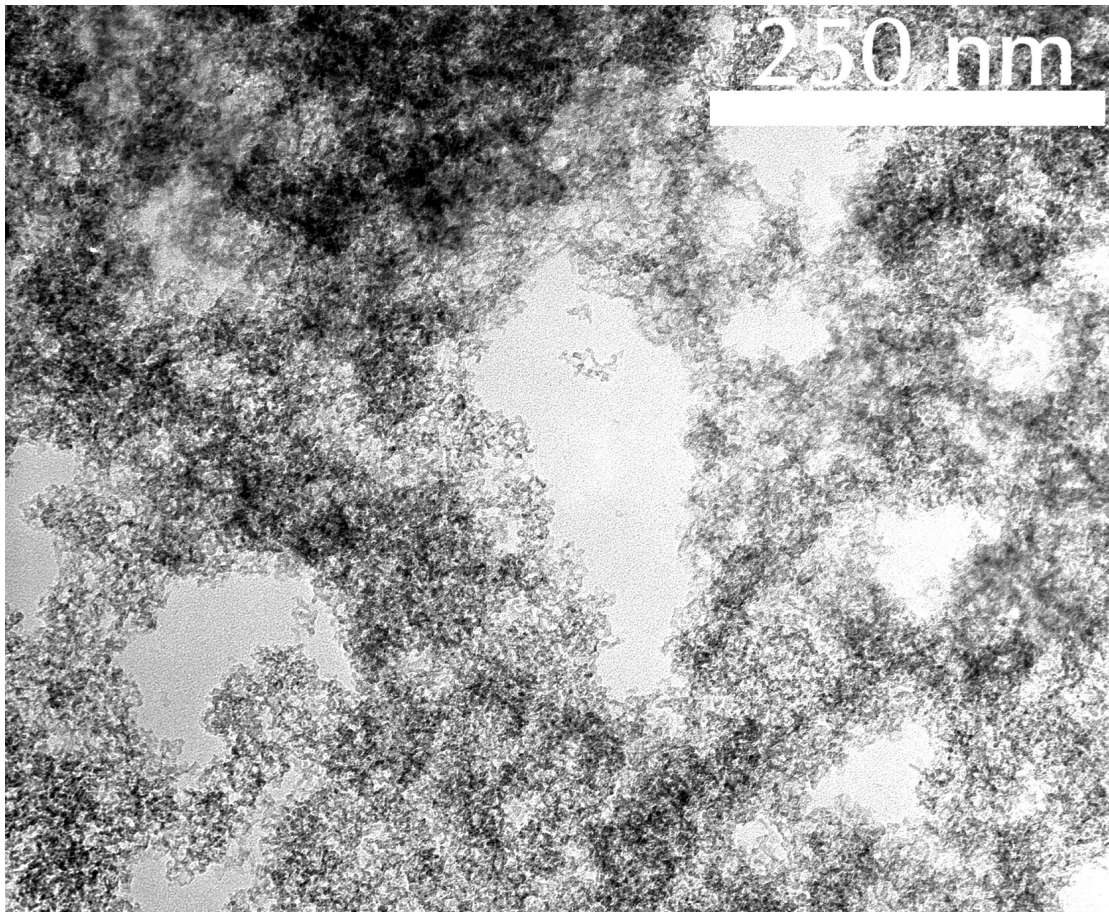


**Figure 3** M. Ayers, et al. UP↑



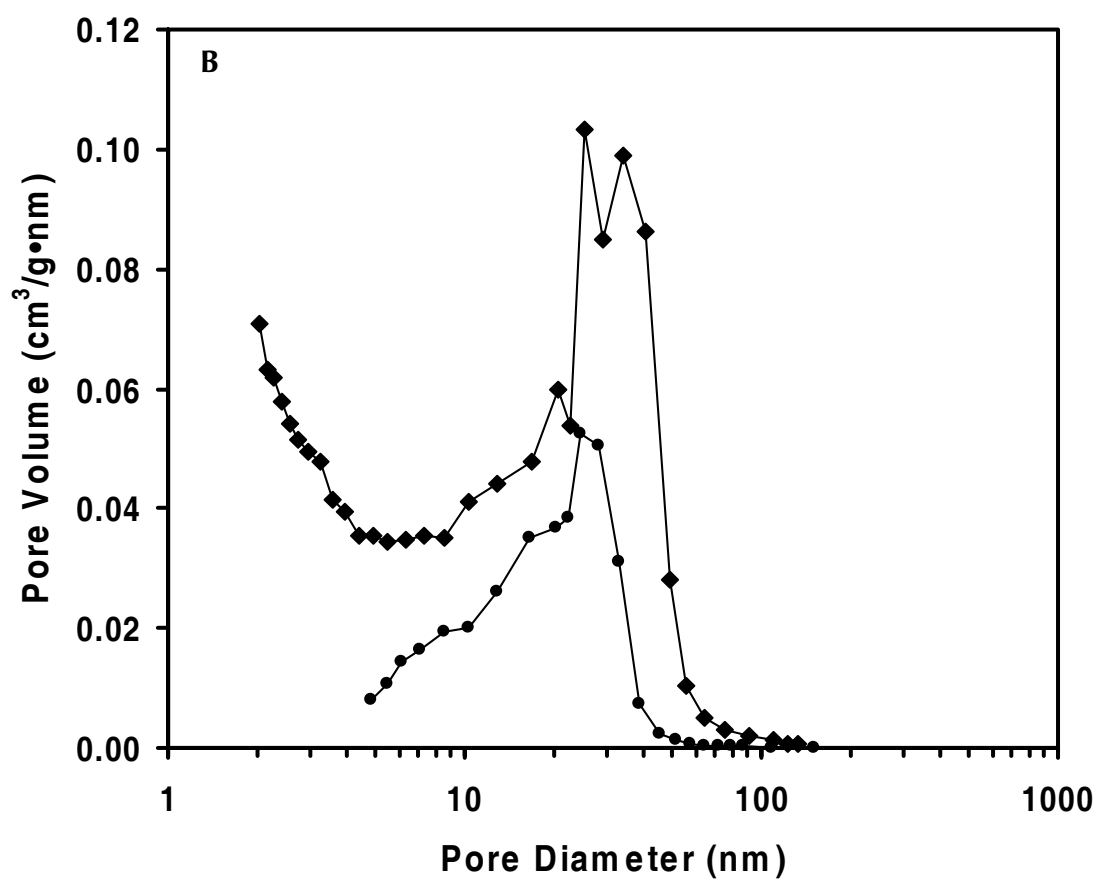
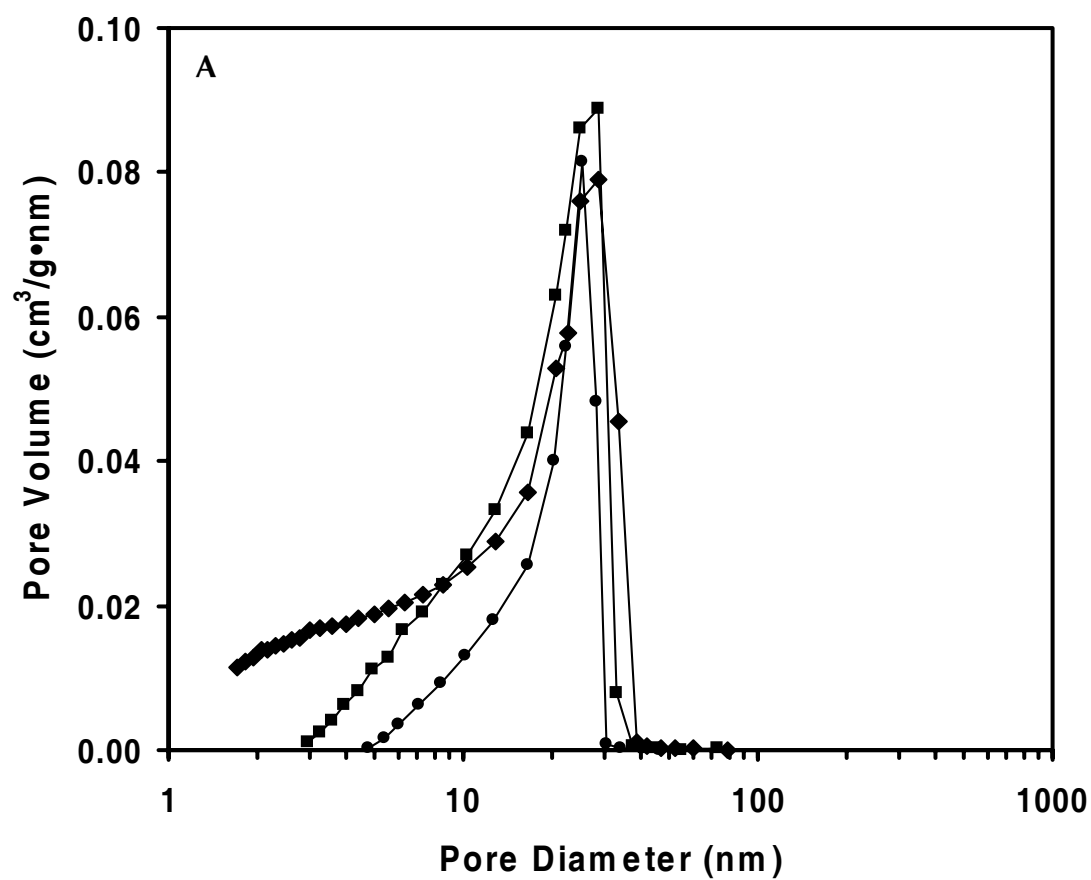


Figure 4 a & b M. Ayers, et al. UP↑

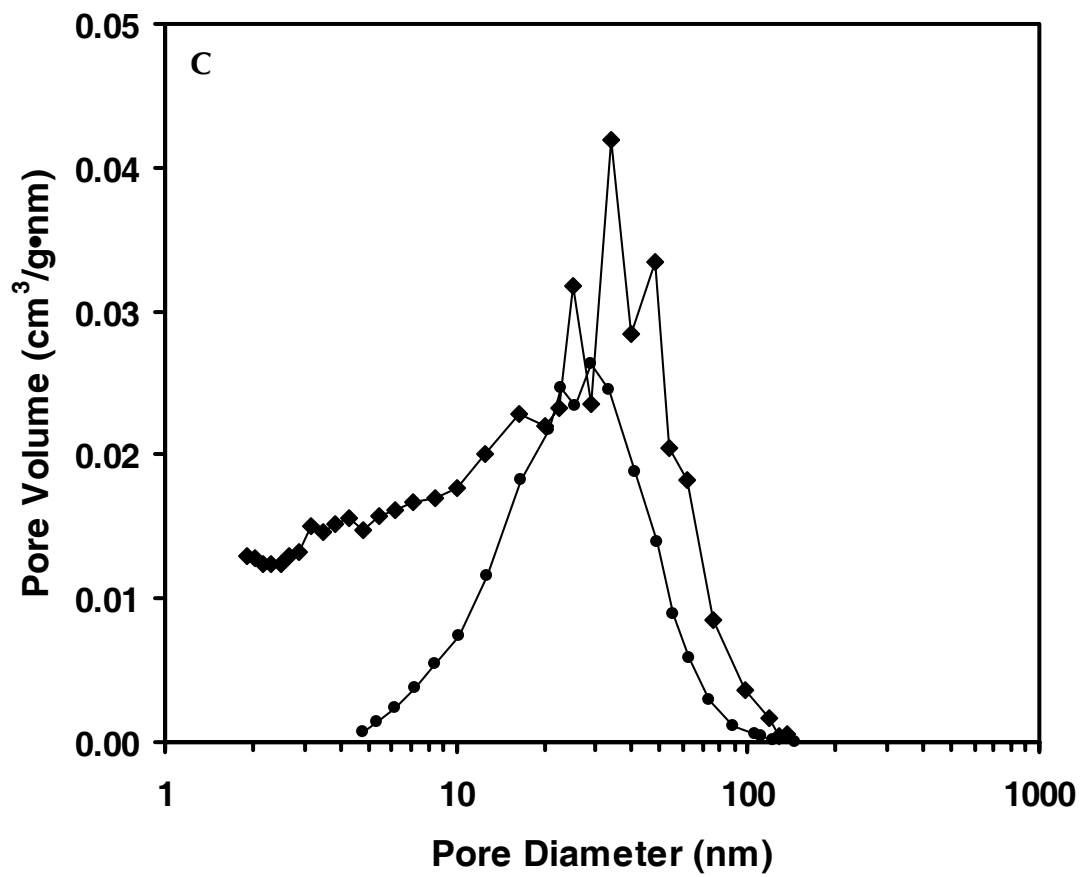
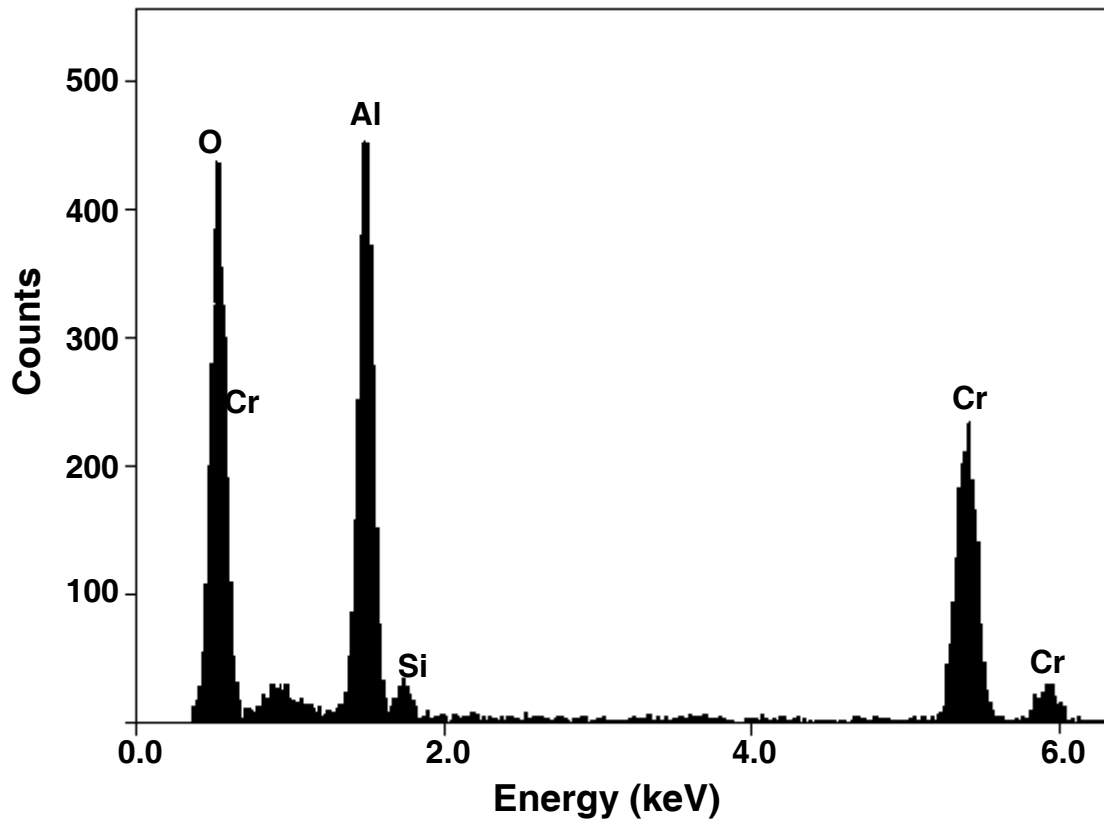
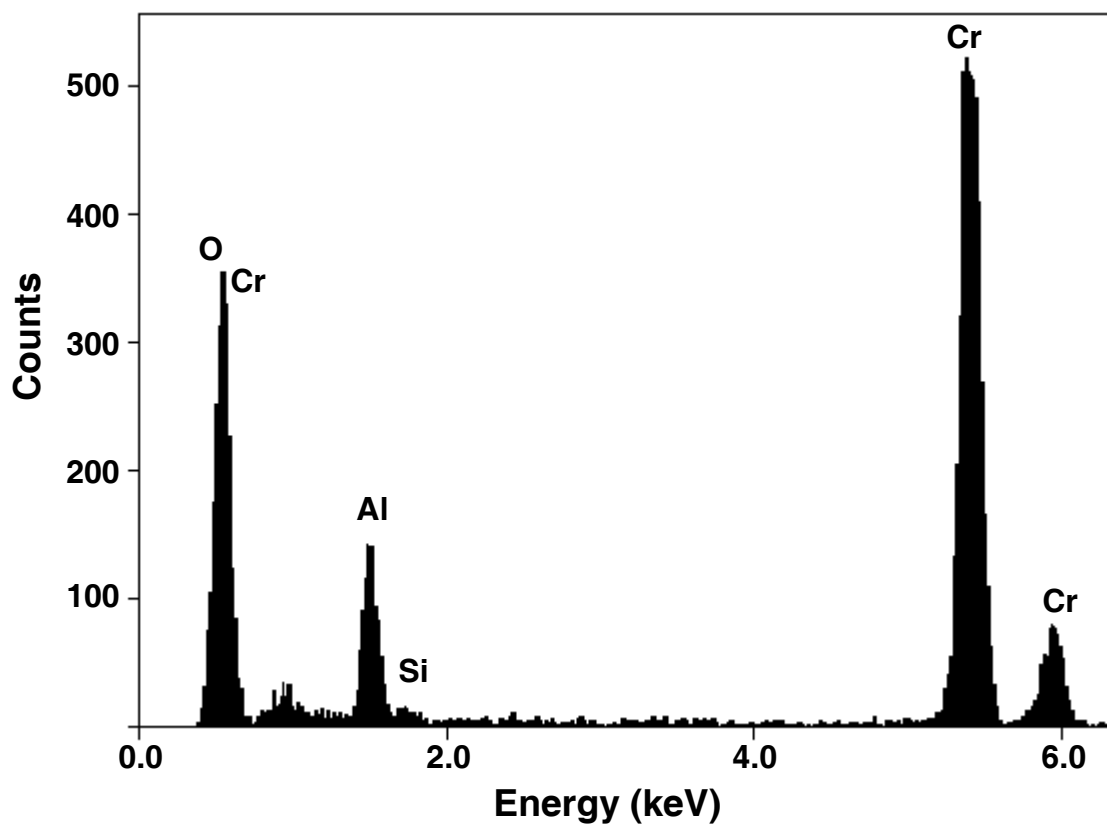
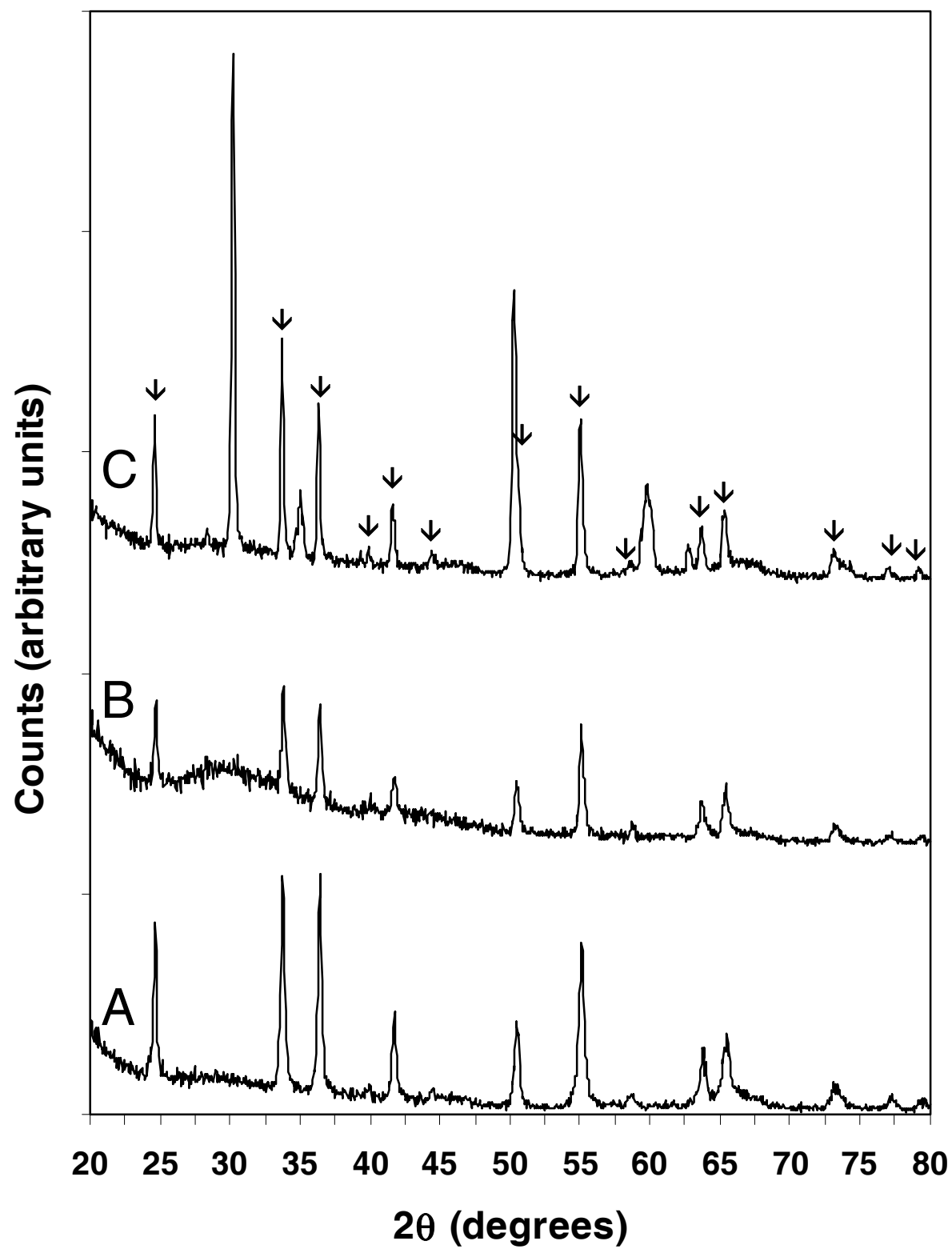


Figure 4 c M. Ayers, et al. UP↑



**Figure 5** M. Ayers, et al. UP↑



**Figure6** M. Ayers, et al. UP↑

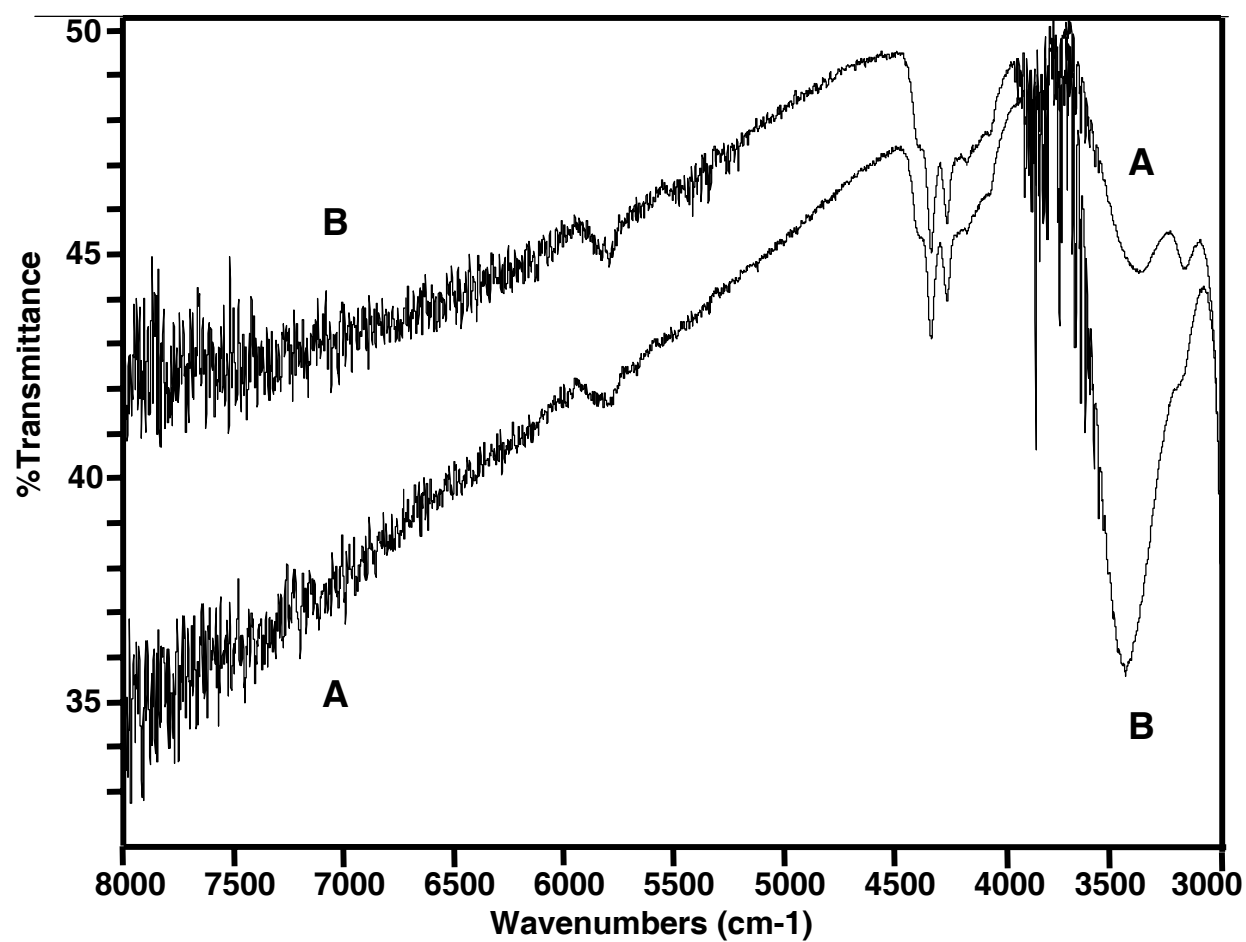


**Figure7** M. Ayers, et al. UP↑